PHYSICAL REVIEW B **74**, 100501(R) (2006)

Momentum densities, Fermi surfaces, and their temperature dependences in Sr_2RuO_4 studied by Compton scattering

N. Hiraoka,[1,*] T. Buslaps,[1] V. Honkimäki,[1] T. Nomura,[2] M. Itou,[3] Y. Sakurai,[3] Z. Q. Mao,[4] and Y. Maeno[4]
[1]*European Synchrotron Radiation Facility (ESRF), Boîte Postale 220, 38043 Grenoble Cedex 9, France*
[2]*Japan Atomic Energy Agency (JAEA/SPring-8), Koto 1-1-1, Sayo, Hyogo 679-5198, Japan*
[3]*Japan Synchrotron Radiation Research Institute (JASRI/SPring-8), Koto 1-1-1, Sayo, Hyogo 679-5198, Japan*
[4]*Department of Physics, Kyoto University, Kyoto 606-8502, Japan*
and Japan CREST, Japan Science and Technology Corporation, Kawaguchi, Saitama 332-0012, Japan
(Received 3 February 2006; published 7 September 2006)

We have measured Compton profiles of Sr_2RuO_4 at 20 K and room temperature to investigate electron momentum densities, Fermi surfaces, and their temperature dependences. Two-dimensional momentum densities have been reconstructed from nine Compton profiles. The Fermi surface signals are observed in the first derivative of the occupation densities in k space, obtained by folding the momentum densities into the first Brillouin zone. The data at $T=20$ K exhibit Fermi surface signals that reasonably agree with those obtained from band theory. On the other hand, the data at room temperature show the signals strongly suppressed due to temperature. This thermal behavior is not understood using band theory based on the local density approximation, implying the importance of electron correlation in the temperature effect.

DOI: 10.1103/PhysRevB.74.100501 PACS number(s): 74.70.Pq, 72.15.−v, 71.18.+y, 78.70.Ck

The perovskite ruthenate Sr_2RuO_4 shows unconventional superconductivity below $T_c=1.5$ K.[1] The Cooper pairs have spin-parallel coupling that prohibits the possibility of s-wave or d-wave symmetry, which are widely believed to appear in conventional or cuprate superconductors. Many theoretical and experimental studies have been carried out on the superconducting state, particularly in order to reveal the Cooper pair coupling symmetry and the coupling mechanism (see Ref. 2). However, superconductivity at low temperature is not the only unusual property of this material. Electron transport at high temperature also appears to be unusual. Although the resistivity in the ab plane is always metallic and monotonically increases with rising temperature as in ordinary metals,[3] the observed Hall resistivity is anomalous. The Hall coefficient changes sign twice between T_c and room temperature (RT).[4] Furthermore, the broad peak at ~130 K of the c-axis resistivity indicates an anomalous behavior. These thermal behaviors are not fully understood yet,[5,6] and so far only few experiments address this issue.

An angle-resolved photoemission spectroscopy (ARPES) experiment has been carried out as a function of temperature.[7] It has been found that the spectral line shape of the electrons (quasiparticles) on the Fermi surfaces (FSs) shows a well-defined peak at low temperature. However, it exhibits a substantial broadening as the temperature increases, with anisotropic behavior. Since ARPES is inherently sensitive to the sample surface (even if x rays of several hundred eV are used), special care is necessary for interpretation of the data as a function of temperature. Even the surface degradation can depend on the temperature. Therefore it would be valuable if ARPES data could be confirmed by a bulk-sensitive method.

Within the impulse approximation,[8] the energy spectrum of Compton-scattered x rays provides the electron momentum density $n(\mathbf{p})$ projected on the scattering vector (p_z axis),[9] namely, the Compton profile (CP),

$$J(p_z) = \int\int n(\mathbf{p})dp_x dp_y. \quad (1)$$

The FS is defined as the boundary between occupied states and unoccupied states in momentum or wave-vector (k) space. Therefore, the derivative of $n(\mathbf{p})$, or, more precisely, the derivative of the occupation densities in k space that is obtained by folding $n(\mathbf{p})$ into the first Brillouin zone,[10] provides the FS geometry in principle. The unique advantage of this technique is that it is not limited by the quality of the sample (e.g., impurity) or the quality of the surface (e.g., oxidation). High-energy x rays, of approximately 100 keV, have a penetration depth as large as 100–1000 μm, and probe the real bulk properties. Although each CP only provides one-dimensional information along the p_z axis, the three- or two-dimensional electron momentum densities can be determined using a numerical reconstruction method from several CPs, which are obtained along different crystallographic orientations.

In the present study, we have measured nine CPs between the [100] axis (Γ-M) and the [110] axis (Γ-X) at $T=20$ K and RT. Two-dimensional momentum densities projected onto the (001) plane have been obtained using a reconstruction method. The data at $T=20$ K exhibit signals reasonably representing the FS geometry. On the other hand, the data at RT show signals suffering from strong thermal broadening, which is not explained by band theory based on the local density approximation (LDA). This study is also important because it shows the feasibility of mapping of FSs in a strongly correlated system using Compton scattering. This success will open the possibility of FS studies of this type of material using this technique.

The sample, having a size of $3\times5\times15$ mm^3, was prepared with the floating zone method. The data at RT were collected using a Cauchois-type spectrometer on beamline BL08W at SPring-8.[11,12] The incident energy (E_0) was

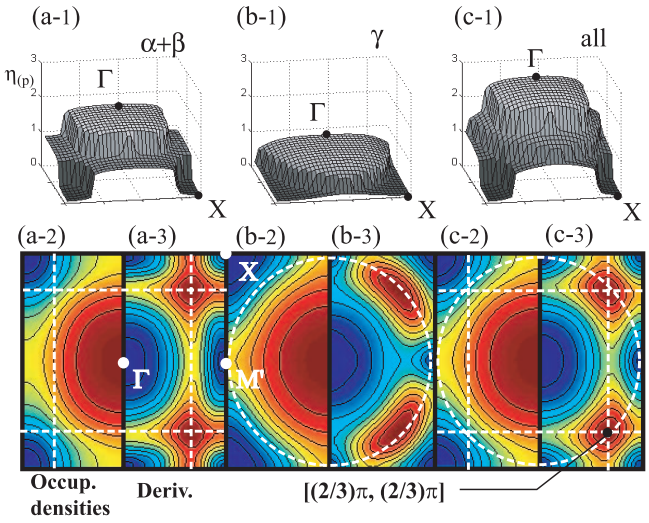

FIG. 1. (Color) Two-dimensional occupation densities (a2), (b2), and (c2) and their first derivatives (a3), (b3), and (c3), reconstructed from nine theoretical Compton profiles which are computed using the Hubbard model (a1), (a2), and (a3). (a) $\alpha+\beta$ FSs, (b) γ FS, and (c) all the FSs ($\alpha+\beta+\gamma$). M' stands for $(\pi,0)$, which is slightly away from the high-symmetry point M.

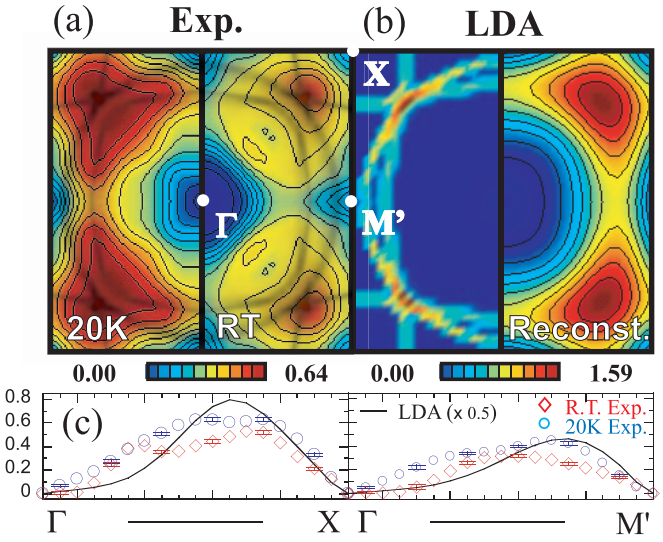

FIG. 2. (Color) (a) Derivatives of experimental occupation densities at $T=20$ K and RT. The FSs determined by ARPES are overlaid (dark shadows). Color scales are the same for the $T=20$ K and RT data. (b) Derivatives of occupation densities from the LDA band theory. The left (right) side is the derivative of the original (reconstructed) occupation densities. (c) Sections along Γ-X (M'). The error bars providing the propagation of statistical errors were obtained from numerical simulations with the LDA CPs and random numbers (see Ref. 26).

115.5 keV. Using the same sample, the data at 20 K were collected with a dispersion-compensation-type spectrometer on beamline ID15B at ESRF with $E_0=88.3$ keV.[13] For the two experimental setups, the momentum resolutions were approximately the same, ~0.13 atomic units (1 a.u. $=1.99\times10^{-24}$ kg m s$^{-1}=1.89$ Å^{-1}). In both experiments, nine CPs were measured along the same directions between [100] and [110] at an angular interval of ~5.6°. The direct Fourier method[14] was used for the reconstructions of the momentum densities. The occupation densities were then obtained by folding the momentum densities into the first Brillouin zone based on the Lock-Crisp-West method.[10] It is shown in Ref. 15 how each procedure transforms data on a similar sample.

In order to analyze the influence of temperature and correlation in the electronic properties, two different theoretical calculations have been carried out. The first is a LDA-based band theoretical calculation. Self-consistent wave functions were determined with the full-potential augmented plane wave method.[31] The other one is a Hubbard model calculation incorporating electron correlation by second-order perturbation theory.[16] The parameters are fixed in such a way that the transport properties at low temperature are reproduced well ($U=4.0$, $U'=J=J'=0.33U$; see Refs. 17 and 18 for the definition of the notation). For both of the calculations, CPs were first computed from the obtained momentum densities based on Eq. (1), and then the two-dimensional momentum densities were reconstructed and folded back in the same way as in the procedure for the experimental data.

Before discussing the experimental data, we demonstrate how the reconstruction procedure reveals the momentum densities and the FSs using the theoretical results obtained from the Hubbard model. (In this case the momentum density is equivalent to the occupation density.) Figure 1 shows the original momentum densities [Figs. 1(a1), 1(b1), and 1(c1)], the reconstructed momentum densities [Figs. 1(a2), 1(b2), and 1(c2)], and their first derivatives [Figs. 1(a3), 1(b3), and 1(c3)]. Here, the broadening effect due to the experimental resolution is included as a filtering function during the reconstructions. The FSs of Sr_2RuO_4 consist of three sheets.[19–25] Hybridized Ru $4d_{xz}$ and $4d_{yz}$ orbitals make two two-dimensional FSs, i.e., a hole pocket around Xs, called the α sheet, and an electron pocket around Γ, called

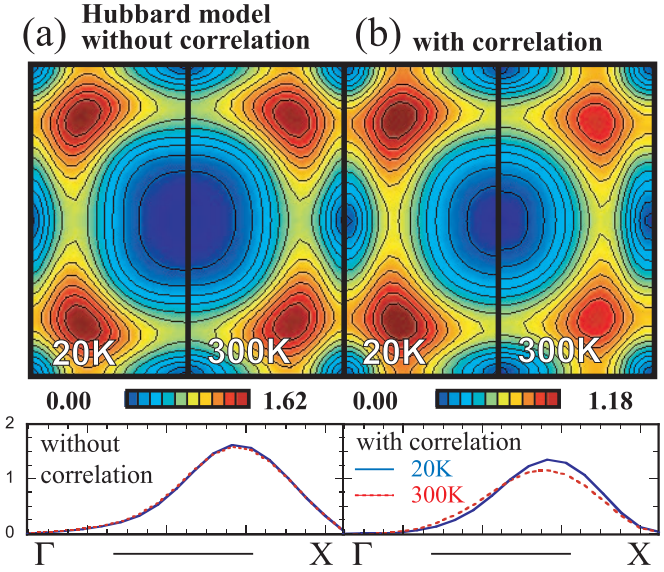

FIG. 3. (Color) Derivatives of the occupation densities obtained from the Hubbard model calculations with (without) electron correlation. The lower panels show sections along Γ-X.

the β sheet [see the white, broken lines in Figs. 1(a2) and 1(a3)]. On the other hand, the $4d_{xy}$ orbital makes a round electron pocket centered at Γ, called the γ sheet [Figs. 1(b2) and 1(b3)]. The reconstructed momentum densities have a rather large broadening, but α and β are still recognized. However, since γ is larger it connects with γ in a second Brillouin zone at $(\pi,0)$ (M'). Therefore it is difficult to find a clear signature of γ along the [100] axis [see Figs. 1(c2) and 1(c3)].

Figure 2(a) shows the first derivatives of the occupation densities reconstructed from the experimental data. For comparison, the FSs determined[23] by ARPES are overlaid on our data (dark shadow). The LDA theoretical ones are also shown in Fig. 2(b). Here, the left side is directly obtained from the LDA calculation, while the right one is reconstructed from the theoretical CPs. It should be noted that the occupation densities are dominated by FS signals, and other effects such as oscillation structures due to Ru $4d-$O $2p$ covalent bonds[15,27] are not discernible. Generally, the LDA does not correctly describe electronic structures in strongly correlated systems. However, it is shown by de Haas–van Alphen experiments and ARPES studies that the FSs of Sr_2RuO_4 are reproduced fairly well by the LDA.[21–25] Therefore it is important to see how our data are interpreted by the LDA band theory. The $T=20$ K data basically agree with the LDA band theory. Both show a strong intensity at $(2/3\pi,2/3\pi)$, where the three FSs intersect. However, some differences are recognized. The first is the intensities of the experimental data, which are less than half of those from the LDA band theory. The second is the more complicated structure of the components at $(2/3\pi,2/3\pi)$ in the $T=20$ K data, appearing to have several structures along the Γ-X axis (see the lower panels). These differences will be discussed along with the RT data afterward.

The RT data suffer from strong thermal broadening. It is difficult to recognize the FS geometry. From the point of view of band theory, the temperature effect on FSs arises from thermal excitations of electrons in the vicinity of the Fermi level. The thermal broadening in momentum space (Δk) is given by $\Delta k=(dE/dk)^{-1}\Delta E=v_F^{-1}\Delta E$, where v_F is the Fermi velocity. ΔE is typically given by the full width at half maximum (FWHM) of the derivative of the Fermi-Dirac function.[32] Using v_F, which is found to be $\sim 4\times 10^5$ m s^{-1} in the band structure diagram (along Γ-X), Δk is evaluated to be 4×10^{-26} kg m s^{-1} ~ 0.04 Å^{-1} ~ 0.02 a.u. This is about six times smaller than the experimental resolution (0.13 a.u.), and it is unlikely that this effect could explain the strong thermal broadening in the RT data.

In the following we will argue that the strong thermal smearing can be explained by electron correlation. Figure 3 shows the correlation effect on the temperature dependence of the FS signals, simulated with Hubbard model calculations. The temperature dependence is very small if the correlation is turned off [Fig. 3(a)], while it becomes noticeable if the correlation is turned on [Fig. 3(b)]. The temperature effect due to the correlation is still much smaller than the experimental data show. Even though this suggests that our model is insufficient to reach a definite conclusion, we might infer the following scenario. It is well known that, as the electron correlation becomes stronger, (i) the coherent part forming FSs is suppressed while the incoherent part is enhanced, and (ii) the bandwidth of the coherent part near the Fermi level is reduced, and therefore v_F is also reduced. These are the reasons why the FS signals are suppressed even at low temperature while the thermal broadening (given by $v_F^{-1}\Delta E$) is enhanced in our model. In the present model, each bandwidth is reduced by a factor of 2–3 when the correlation is turned on. However, our model might still underestimate the reduction of the bandwidths. This could be the reason for the smaller temperature effect. The first difference that was found between the experiment and the LDA band theory was a considerable reduction of the FS signals in the $T=20$ K data. This scenario could explain this fact as well as the significant smearing of FS signals in the RT data.

Many theoretical studies report that the LDA band structure for Sr_2RuO_4 has Van Hove singularities (VHSs) 60 meV above the Fermi level near the M points. If the band dispersions can be rescaled by a factor of 2–3 due to correlation, a major part of the electrons should be excited into VHSs for temperatures above 100 K. The rescaling factor for these VHSs might be even larger since they are derived from the band having the heaviest electron mass of the three FSs (γ).[21,22] Therefore, one could effectively consider that Sr_2RuO_4 has two kinds of FS geometries when transport properties are discussed at high temperature: One consists of two electron sheets and one hole sheet as the ground state (the real one), and the other consists of one electron sheet and two hole sheets as the excited state (the virtual one).

The discussion above partly explains the temperature dependence in the experimental data. However, the difference that is seen between the $T=20$ K experimental data and the RT ones is more complicated. They differ not only in the intensities but also in the topologies, contrary to the Hubbard model calculations. As already mentioned, the components at $(2/3\pi,2/3\pi)$ in the $T=20$ K data show a more complex structure, which looks as if the β FS signals (inner parts) were separated from the α and γ ones (outer parts). In the RT data, the inner parts appear to be suppressed much more than the outer ones. The present Hubbard model calculations do not show such suppression of the specific FS signals. The origin of this behavior is still unclear. It may be due to electron correlation that is not described by our present theoretical calculations. Our model has actually been developed in order to describe the transport property at low temperature, i.e., the electronic structure in a quite narrow energy range near the Fermi level.[16–18] However, the theory needs to be valid in a wider range of binding energy to reproduce Compton scattering data since this technique observes all the electrons in the sample. Such a theory has not been well established yet despite many efforts of theorists so far. Another issue to be addressed is the validity of the impulse approximation, i.e., the validity of Eq. (1). If high-energy x rays around 100 keV are used, the impulse approximation is generally valid for experiments with the present resolution.[28] However, it is worth investigating the scattering process in strongly correlated electron systems without making the impulse approximation.[29,30]

In summary, we have measured CPs of Sr_2RuO_4 at 20 K and RT in order to investigate the momentum densities, the occupation densities in k space, the FSs, and their thermal behaviors. FS signals were observed in the first derivative of the occupation densities, reconstructed from the CPs. The signals representing the FS geometry were observed in the data at 20 K. The FS signals observed in the $T=20$ K data were structured more than the theories predicted. On the other hand, those signals in the RT data were strongly suppressed. Furthermore, the specific FS signals that could be assigned to the β sheet were largely suppressed. The origins of these effects should be clarified by further theoretical studies.

We would like to thank Y. Tanaka for providing us the reconstruction program. The experiment at 20 K was carried out under ESRF Proposal No. BLC1386, and the experiment at RT was done under SPring-8 Proposal No. 2001B0497-ND-np. This work was financially supported by a Grant-in-Aid for Scientific Research (Grant No. 18340111) from the Ministry of Education, Culture, Sports, Science and Technology.

*Present address: NSRRC, Hsinchu 30076, Taiwan. Electronic address: hiraoka@spring8.or.jp

[1] Y. Maeno, H. Hashimoto, K. Yoshida, S. Nishizaki, T. Fujita, J. G. Bednorz, and F. Lichtenberg, Nature (London) **372**, 532 (1994).
[2] A. P. Mackenzie and Y. Maeno, Rev. Mod. Phys. **75**, 657 (2003).
[3] N. E. Hussey, A. P. Mackenzie, J. R. Cooper, Y. Maeno, S. Nishizaki, and T. Fujita, Phys. Rev. B **57**, 5505 (1998).
[4] A. P. Mackenzie, N. E. Hussey, A. J. Diver, S. R. Julian, Y. Maeno, S. Nishizaki, and T. Fujita, Phys. Rev. B **54**, 7425 (1996).
[5] C. Noce and M. Cuoco, Phys. Rev. B **59**, 2659 (1999).
[6] I. I. Mazin, D. A. Papaconstantopoulos, and D. J. Singh, Phys. Rev. B **61**, 5223 (2000).
[7] S. C. Wang *et al.*, Phys. Rev. Lett. **92**, 137002 (2004).
[8] P. Eisenberger and P. M. Platzman, Phys. Rev. A **2**, 415 (1970).
[9] M. J. Cooper, Rep. Prog. Phys. **48**, 415 (1985).
[10] D. G. Lock, V. H. C. Crisp, and R. N. West, J. Phys. F: Met. Phys. **3**, 561 (1973).
[11] N. Hiraoka, M. Itou, T. Ohata, M. Mizumaki, Y. Sakurai, and N. Sakai, J. Synchrotron Radiat. **8**, 26 (2001).
[12] M. Itou and Y. Sakurai, in *Eighth International Conference on Synchrotron Radiation Instrumentation*, edited by T. Warwick, J. Arthur, H. A. Padmore, and J. Stöhr, AIP Conf. Proc. No. 705 (AIP, Melville, NY, 2004), p. 901.
[13] N. Hiraoka, T. Buslaps, V. Honkimäki, and P. Suortti, J. Synchrotron Radiat. **12**, 670 (2005).
[14] Y. Tanaka, Y. Sakurai, A. T. Stewart, N. Shiotani, P. E. Mijnarends, S. Kaprzyk, and A. Bansil, Phys. Rev. B **63**, 045120 (2001).
[15] N. Hiraoka, T. Buslaps, V. Honkimäki, H. Minami, and H. Uwe, Phys. Rev. B **71**, 205106 (2005).
[16] T. Nomura and K. Yamada, J. Phys. Soc. Jpn. **69**, 3678 (2000).
[17] T. Nomura and K. Yamada, J. Phys. Soc. Jpn. **71**, 1993 (2002).
[18] T. Nomura and K. Yamada, J. Phys. Chem. Solids **63**, 1337 (2002).
[19] T. Oguchi, Phys. Rev. B **51**, 1385 (1995).
[20] D. J. Singh, Phys. Rev. B **52**, 1358 (1995).
[21] A. P. Mackenzie, S. R. Julian, A. J. Diver, G. J. McMullan, M. P. Ray, G. G. Lonzarich, Y. Maeno, S. Nishizaki, and T. Fujita, Phys. Rev. Lett. **76**, 3786 (1996).
[22] Y. Yoshida, R. Settai, Y. Ōnuki, H. Takei, K. Betsuyaku, and H. Harima, J. Phys. Soc. Jpn. **67**, 1677 (1998).
[23] A. Damascelli *et al.*, Phys. Rev. Lett. **85**, 5194 (2000).
[24] C. Bergemann, S. R. Julian, A. P. Mackenzie, S. NishiZaki, and Y. Maeno, Phys. Rev. Lett. **84**, 2662 (2000).
[25] A. Sekiyama *et al.*, Phys. Rev. B **70**, 060506(R) (2004).
[26] N. Hiraoka, T. Buslaps, V. Honkimäki, H. Guyot, and C. Schlenker, Phys. Rev. B **71**, 125417 (2005).
[27] N. Hiraoka, A. Deb, M. Itou, Y. Sakurai, Z. Q. Mao, and Y. Maeno, Phys. Rev. B **67**, 094511 (2003).
[28] J. A. Soininen, K. Hämäläinen, and S. Manninen, Phys. Rev. B **64**, 125116 (2001).
[29] I. G. Kaplan, B. Barbiellini, and A. Bansil, Phys. Rev. B **68**, 235104 (2003).
[30] B. Barbiellini and A. Bansil, J. Phys. Chem. Solids **65**, 2031 (2004).
[31] A. Kodama, N. Hamada, and A. Yanase, Computer code BANDS01, Fuji Research Inst. Corp. See, e.g., M. Umekawa *et al.*, J. Phys. Soc. Jpn. **73**, 430 (2004) for details of the calculation.
[32] ΔE is given by $\ln(\sqrt{8}+3)k_BT$. Note that a factor of $\ln(\sqrt{8}+3)$ is necessary in order to get an exact FWHM.